Acta Cryst. (1992). **B48**, 1–11

Structure and Twinning of Sr_3CuPtO_6

By J. L. Hodeau, H. Y. Tu,* P. Bordet, T. Fournier,† P. Strobel and M. Marezio‡

Laboratoire de Cristallographie, CNRS, associé à l'Université J. Fourier, 166X, 38042 Grenoble CEDEX, France

and G. V. Chandrashekhar

IBM Research Division, T. J. Watson Research Center, Yorktown Heights, NY 10598, USA

(*Received 12 March 1991; accepted 21 August 1991*)

Abstract

Sr_3CuPtO_6 was obtained during the investigation of the Bi–Sr–Cu–O system in Pt crucibles. The reaction with Pt gives rise to large platelets of mixed phases. The new phase Sr_3CuPtO_6 reported here has a well defined composition and its structure is related to that of other Pt^{4+} compounds. The solution and refinement of the structure were based on single-crystal X-ray diffraction data at room temperature. The symmetry is monoclinic, space group *C*2/*c* with $Z = 4$, $a = 9.317$ (4), $b = 9.720$ (4), $c = 6.685$ (3) Å, $\beta = 91.95$ (2)°, $V = 605.1$ (8) Å^3, $M_r = 617.49$, $D_x = 6.778$ g cm^{-3}, $\mu = 282.1$ cm^{-1}, $F(000) = 1076$, room temperature. Monochromatized Ag $K\alpha$ radiation ($\lambda = 0.56083$ Å) was used. The final refinement gave an *R* factor of 0.048 for 582 independent reflections. Owing to the presence of more than one pseudo-symmetry in the lattice of Sr_3CuPtO_6, all the crystals were heavily twinned. The possible twinning laws were investigated and a correction which eliminated the effect of twinning was applied. The structure contains chains alternating a PtO_6 octahedron and a CuO_4 'square' which share edges. They are connected by Sr sites in eightfold coordination. The Pt cations are surrounded by a nearly perfect O octahedron and Cu cations by six O atoms arranged as a distorted trigonal prism with four short and two long Cu—O distances. The Cu cations are displaced towards one of the rectangular faces of the prism and can be considered to have square coordination. The structure of Sr_3CuPtO_6 is related to that of trigonal Sr_4PtO_6. Chemical analysis of various platelets indicated the presence of intergrowth between Bi/Sr/Cu and Pt/Sr/Cu phases. However, no Bi/Pt substitution occurs in any phase. The microanalysis revealed that the surface of the crystal studied by X-rays did not contain any Bi. All Sr_3CuPtO_6 crystals are twinned either by reticular pseudo-merohedry with a pseudo-orthorhombic cell and/or by pseudo-merohedry with a pseudo-rhombohedral cell. A detailed twinning analysis is given; it allows comparison of the symmetry of Sr_3CuPtO_6 with those occurring in other $M_4^{2+}PtO_6$ compounds.

Introduction

The Bi–Sr–Ca–Cu–O system has been studied extensively because it includes the series of the superconductors $Bi_2Sr_2Ca_{n-1}Cu_nO_x$ (Maeda, Tanaka, Fukutomi & Asano, 1988; Akimitsu, Yamazaki, Sawa & Fujiki, 1988; Michel, Hervieu, Borel, Grandin, Deslandes, Provost & Raveau, 1987; Roth, Rawn, Burton & Beech, 1990*a*). Various phase-diagram studies showed that a large number of intermediate compounds exist in the Bi_2O_3–SrO–CuO triangular composition (Roth, Rawn, Burton & Beech 1990*a*,*b*; Saggio, Sujata, Hahn, Hwu, Poeppelmeier & Mason, 1989; Ikeda, Ito, Shimomura, Oue, Inaba, Hiroi & Takano, 1989; Roth, Rawn & Bendersky, 1990). In addition, crystal growth attempts in Pt crucibles showed that at high temperatures a reaction with the container could occur, giving rise to Pt-containing compounds (Strobel, Kelleher, Holtzberg & Worthington, 1988). It is this chemical attack on the Pt crucibles which led to the investigations of the possible reactions between Pt and the alkaline-earth oxide (Randall & Katz, 1959; Randall & Ward, 1969). Generally, Pt-based oxides contain either Pt^{2+} in fourfold planar coordination or octahedral Pt^{4+} cations. For example, the oxides $M_xPt_3O_4$ contain square-planar PtO_4 groups with Pt^{2+}—O distances of about 2.00 Å (Schwartz & Prewitt, 1984; Schwartz, Prewitt, Shannon, Corliss, Hastings & Chamberland, 1982). Several Pt^{4+} oxides with formulae $M_2^{+}PtO_3$ and $M_4^{2+}PtO_6$ can also be synthesized; the octahedrally coordinated PtO_6 groups share faces, edges or can be isolated (Randall & Katz, 1959; Schwartz & Prewitt, 1984; Ben-Dor,

---

* Permanent address: Shanghai Institute of Ceramics, Academia Sinica, 865 Chang-Ning Road, Shanghai 200050, People's Republic of China.

† Also CRTBT, CNRS, 166X, 38042 Grenoble CEDEX, France.

‡ Also AT&T Bell Laboratories, Murray Hill, NJ 07974, USA.

0108-7681/92/010001-11$03.00

Suss & Cohen, 1983; Chamberland & Silverman, 1979; Schneider & McDaniel, 1969). Mixed-valence ternary Pt oxides MPt_3O_6 present both planar PtO_4 groups (Pt—O distances ≃ 1.94–1.99 Å) and octahedral PtO_6 groups (Pt—O distances ≃ 2.00–2.03 Å) (Schwartz, Parise, Prewitt & Shannon, 1983). In these oxides, the Pt sites are quite rigid, the Pt—O distances vary over a small range and only small angular distortions can occur. The main differences concern the stacking of planar PtO_4 groups and octahedral PtO_6 ones.

During the crystal growth studies of Bi–Sr–Cu–O compounds, we observed the formation of single crystals different from those expected. These crystals having a platelet habit were found to be either Sr_4PtO_6, a known trigonal compound (Randall & Katz, 1959; Ben-Dor *et al.*, 1983) or a new phase closely related to Sr_4PtO_6, but containing Cu as a major consitutuent. We report the structure determination of Sr_3CuPtO_6, a compound not mentioned in the review article by Schwartz & Prewitt (1984). We compared its structure with that of other ternary Pt oxides. Since all Sr_3CuPtO_6 crystals are twinned, a study of the twinning is also presented.

Preparation and chemical analysis

Stoichiometric $Bi_2Sr_2CuO_6$ mixtures with 50% CuO excess, held in Pt crucibles for several hours at 1375 K, then cooled at 1–2 K h^{-1}, yielded large hexagonal plate-shaped crystals corresponding to Pt/Bi–Sr–Cu–O mixed phases. An SEM/EDX characterization of these platelets gave four well defined compositions in the same 'crystal'. These compositions are (in Fig. 1, from dark to light) (*a*) CuO, (*b*) $Sr_{3.08(3)}Cu_{0.99(2)}Pt_{0.92(1)}O_x$, (*c*) $Bi_{1.52(3)}Sr_{2.15(2)}Cu_{1.33(3)}O_x$ and (*d*) $Bi_{2.01(5)}Sr_{1.97(5)}Cu_{1.02(7)}O_x$. The numbers in parentheses are the estimated errors on the last decimal figure. These values are the results of several reproducible analyses. From previous studies of the Bi–Sr–Cu–O system (Saggio *et al.*, 1989; Ikeda *et al.*, 1989; Roth *et al.*, 1990, 1990*a*;

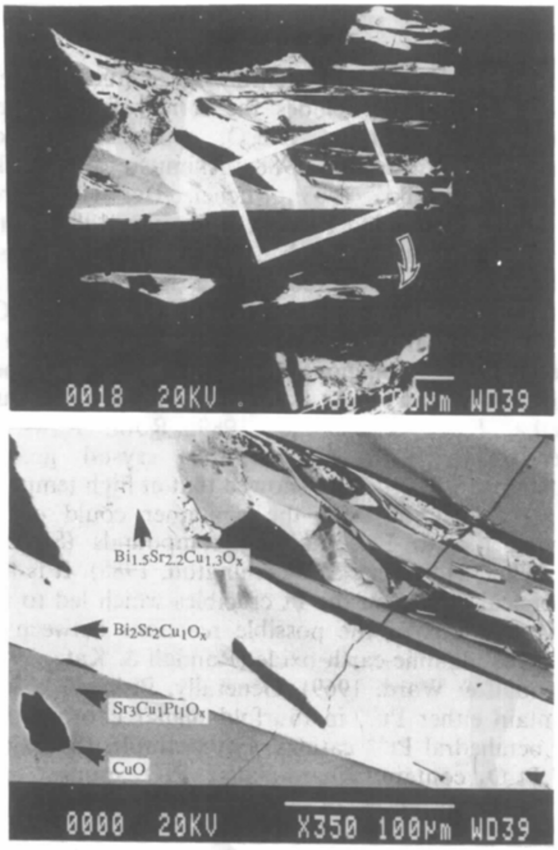

Fig. 1. SEM micrographs of a polished multiphase platelet (entire platelet and enlargement of the same platelet with a different contrast). The bright zones correspond to $Bi_{2.01(5)}Sr_{1.97(5)}Cu_{1.02(7)}O_x$, the light grey to $Bi_{1.52(3)}Sr_{2.15(2)}Cu_{1.33(3)}O_x$, the dark grey to $Sr_{3.08(3)}Cu_{0.99(2)}Pt_{0.92(1)}O_x$ and the black to CuO.

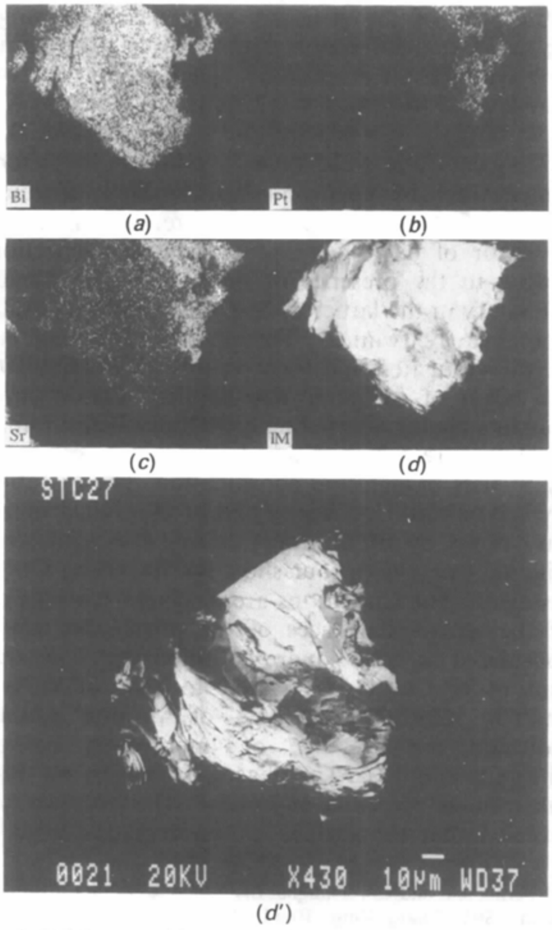

Fig. 2. EDX composition maps of a 'single' crystal characterized by the X-ray precession method: (*a*) Bi content, (*b*) Pt content, (*c*) Sr content, (*d*) and (*d′*) entire crystal.

Strobel *et al.*, 1988), the (*c*) and (*d*) phases were identified as the $Bi_2Sr_3Cu_2O_8$ (Ikeda *et al.*, 1989; Roth *et al.*, 1990*a*) and $Bi_2Sr_2CuO_6$ compounds (Saggio *et al.*, 1989; Roth *et al.*, 1990). Nearly all the 'crystals' contained the (*b*), (*c*) and (*d*) compositions (Fig. 2), but the X-ray precession patterns of these multiphased 'crystals' were similar to those of 'pure' Sr/Cu/Pt/O samples. For example, their lattice parameters were equal (within experimental errors) to those of the Sr/Cu/Pt/O samples and they seemed to belong to the trigonal system. Probably, only the Pt compound is well crystallized while the Bi phases are present in these platelets as amorphous inclusions. As shown in Fig. 1, $Bi_{1.5}Sr_{2.15}Cu_{1.3}O_x$ and $Bi_2Sr_2CuO_x$ are distinct, intimately mixed phases, which probably grew simultaneously with Sr_3CuPtO_x from the high-temperature liquid phase.

Symmetry and twinning

Guinier powder patterns (Table 1) are indexed with a *C*-centered monoclinic cell with parameters $a_0 = 9.317\,(4)$, $b_0 = 9.720\,(4)$, $c_0 = 6.685\,(3)$ Å, $\beta_0 = 91.95\,(2)^\circ$ (Tu, Hodeau, Bordet, Chandrashekhar, Fournier, Strobel & Marezio, 1990). As these 'crystals' can contain either Bi-based or Pt-based phases, the powder pattern reported in Table 1 was obtained by grinding only one 'crystal' containing Pt. This cell indexes 56 of the 59 observed reflections ($I > 5\%\,I_{max}$, $R = 0.1\%$), with absences suggesting *C*2/*c* space-group symmetry. The three unindexed reflections ($d = 3.455$, 2.697 and 2.526 Å) have relative intensities less than 10% of the maximum intensity in the pattern and are ascribed to impurities. Investigations of several crystals with a precession camera and Mo $K\alpha$ radiation (Fig. 3) indicate that the crystals of Sr_3CuPtO_x have pronounced pseudo-rhombohedral metric symmetry as shown by the equivalent cell parameters in Table 2 ($a_2 \simeq 6.716$ Å, $\alpha_2 \simeq 91.7^\circ$), and is also remotely pseudo-cubic, owing to a rhombohedral angle of roughly 92° ($a_1 \simeq 6.713$ Å). The above rhombohedral cell can also be described with the corresponding hexagonal cell ($a_3 \simeq 9.638$, $c_3 \simeq 11.281$ Å) or its equivalent orthohexagonal cell ($a_4 \simeq 9.599$, $b_4 \simeq 16.776$, $c_4 \simeq 11.281$ Å, $\beta_4 \simeq 90.84^\circ$, *C*-centered orthorhombic). Pseudo-orthorhombic, pseudo-rhombohedral and pseudo-cubic indexings of our powder pattern are also given in Table 1. Since the crystal lattice of Sr_3CuPtO_x is consistent with several pseudo-symmetry sublattices, multiple twin formation is very probable.

Since β_0 is almost 90°, the *C*2/*c* lattice (a_0, b_0, c_0, β_0) is consistent with the pseudo-orthorhombic lattice (a_0, b_0, c_0). This gives rise to the possibility of twinning by pseudo-merohedry (Friedel, 1964), controlled by the *mmm* pseudo-symmetry of lattice *Cmcm*. The twin laws predicted by the theory are 2/*m*, 2/*m*. The two mirror planes are parallel to the $(100)_0$ and $(001)_0$ planes and the normals to these planes are the two pseudo-twofold axes. Since the operations of the twofold axes are indistinguishable from the operations of the corresponding equivalent planes, only the planes will be considered in the following discussion.

The pronounced rhombohedral pseudo-symmetry is also a pseudo-symmetry from the structural point of view, as will be shown in *Description of the structure*. Accordingly, the missing rhombohedral symmetry elements can be twin operations, probably with domain formation and are indeed seen on most samples. For those twins by pseudo-merohedry (Friedel, 1964) all reflections due to the different individuals are nearly superimposed because twinning approximately restores all lattice nodes with a slight obliquity of ~0.8°. The twin laws predicted by the theory are the pseudo-threefold axis $[001]_3^{120}$ {which corresponds to $\leftrightarrow [111]_2^{120}$ and $\leftrightarrow [101]_0^{120}$ in the (a_2, b_2, c_2) and (a_0, b_0, c_0) lattices}. This twin law produces spot splittings which are observed in the precession pattern (see Fig. 3*a*).

The (a_0, b_0, c_0, β_0) lattice is also consistent with the pseudo-orthohexagonal sublattice (a_4, b_4, c_4, $\alpha_4 = 89.93$, $\beta_4 = 89.88$, $\gamma_4 = 90.84^\circ$), which has a triple unit-cell volume; the corresponding possibility of twinning is by reticular pseudo-merohedry (Friedel, 1964). The twin laws predicted by the theory in this case are the symmetry elements of this lattice, namely 2/*m*, 2/*m*, 2/*m* [$100_4 \leftrightarrow (\bar{1}12)_0$, $(010)_4 \leftrightarrow (\bar{1}\bar{3}2)_0$, $(001)_4 \leftrightarrow (101)_0$ are the mirror planes and the normals to these planes are the pseudo-twofold axes]. Since two angles of this lattice are very close to 90°, the most probable twinning would be controlled by pseudo-symmetries of the monoclinic lattice (a_4, b_4, c_4, $\alpha_4 = 90$, $\beta_4 = 90$, $\gamma_4 = 90.84^\circ$). The precession patterns given in Figs. 4(*a*) and 4(*b*) show this pseudo-orthorhombic cell ($a \simeq 9.599$, $b \simeq 16.776$, $c \simeq 11.281$ Å, $\alpha \simeq 90$, $\beta \simeq 90$, $\gamma \simeq 90.84^\circ$). The two twinned individuals controlled by the $(001)_4$ twin law can be observed in Fig. 4(*a*).

Intensity data collection

Since all 'crystals' were multi-twinned those with the fewest number of twin individuals were selected by the use of a precession camera for the X-ray data collection. A large fraction of the twin individuals were eliminated by grinding the 'crystals' into spheres. Owing to the habit and the anisotropic hardness of the original crystals, the samples had ellipsoidal shapes after grinding. The size of the ellipsoid used for the intensity data collection was $r_1 = 0.16$, $r_2 = 0.12$, $r_3 = 0.07$ mm. A chemical analysis performed on the surface of this ellipsoid gave a composition close to Sr_3CuPtO_x, *i.e.* without Bi.

Table 1. *Powder data*

		Monoclinic cell*				'Orthorhombic' cell†				Hexagonal cell‡				Rhombohedric cell§				Cubic cell¶			
d_{obs}	I_{obs}	*h*	*k*	*l*	d_{calc}	*h*	*k*	*l*	d_{calc}	*h*	*k*	*l*	d_{calc}	*h*	*k*	*l*	d_{calc}	*h*	*k*	*l*	d_{calc}
4.879	12	0	2	0	4.860	1	−3	0	4.860	1	1	0	4.819	1	0	1	4.819	1	0	−1	4.747
4.805	20	1	1	−1	4.799	−1	−3	0	4.799	2	−1	0	4.819	1	−1	0	4.819	1	−1	0	4.747
4.698	23	1	1	1	4.682	1	−1	2	4.680	0	1	2	4.673	1	1	0	4.674	1	1	0	4.747
4.667	20	2	0	0	4.656	−1	−1	2	4.661	1	−1	2	4.673	1	0	1	4.674	1	0	1	4.747
3.455	4																				
3.371	8	2	2	0	3.362	0	4	2	3.364	2	0	2	3.355	2	0	0	3.355	2	0	0	3.356
3.029	10	2	2	−1	3.033	−1	5	1	3.035	3	1	1	3.038	2	−1	0	3.038	2	−1	0	3.002
2.978	48	2	2	1	2.974	1	−3	3	2.974	1	1	3	2.965	2	1	0	2.965	2	1	0	3.002
		3	1	0	2.957	−1	−3	3	2.960	2	−1	3	2.965	2	0	1	2.965	2	0	1	3.002
		1	1	2	2.963	2	0	3	2.960	−1	2	3	2.965	1	2	0	2.965	1	2	0	3.002
2.799	100	1	3	−1	2.794	0	−6	0	2.794	3	0	0	2.782	2	−1	−1	2.782	2	−1	−1	2.741
2.762	60	2	0	2	2.759	−3	3	0	2.759	3	−3	0	2.782	1	−2	1	2.782	1	−2	1	2.741
		1	3	1	2.770	2	4	2	2.770	1	2	2	2.753	2	1	−1	2.753	2	1	−1	2.741
		0	2	2	2.753	1	−5	−2	2.751	3	−1	−2	2.753	1	−2	−1	2.753	1	−2	−1	2.741
2.740	5	3	1	−1	2.737	2	−4	2	2.739	3	2	2	2.753	2	1	1	2.753	2	−1	1	2.741
2.697	9																				
2.675	16	3	1	1	2.672	0	−2	4	2.673	1	0	4	2.672	2	1	1	2.672	2	1	1	2.741
		2	0	2	2.671	1	1	4	2.669	−1	1	4	2.672	1	2	1	2.672	1	2	1	2.741
2.526	3																				
2.405	3	2	2	2	2.399	2	−6	0	2.399	4	−2	0	2.409	2	−2	0	2.409	2	2	0	2.373
2.342	33	2	2	2	2.341	2	2	4	2.340	0	2	4	2.337	2	2	0	2.337	2	2	0	2.373
2.327	20	4	0	0	2.328	−2	−2	4	2.331	2	−2	4	2.337	2	0	2	2.337	2	0	2	2.373
2.285	9	0	4	−1	2.284	1	−7	−1	2.283	3	1	1	2.268	2	−1	−2	2.268	2	−1	−2	2.238
2.254	6	3	1	−2	2.251	−3	5	1	2.252	4	−3	1	2.268	2	2	1	2.268	2	2	1	2.238
2.157	11	2	4	0	2.154	1	−7	2	2.155	3	1	2	2.142	3	0	−1	2.142	3	0	1	2.123
2.142	15	3	3	−1	2.141	1	7	2	2.142	4	1	2	2.142	3	−1	0	2.142	3	1	0	2.123
2.131	8	1	1	3	2.130	−3	5	−2	2.128	4	−3	−2	2.142	1	3	0	2.142	1	−3	0	2.123
2.112	20	3	3	1	2.109	1	−5	4	2.110	2	1	4	2.103	3	1	0	2.103	3	1	0	2.123
2.101	35	4	2	0	2.099	−1	−5	4	2.101	3	−1	4	2.103	3	0	1	2.103	3	0	1	2.123
		1	1	3	2.099	3	1	4	2.096	−2	3	4	2.103	1	3	0	2.103	1	3	0	2.123
2.041	18	2	4	1	2.041	2	−6	3	2.041	2	2	3	2.029	3	1	1	2.029	3	1	−1	2.024
2.027	30	0	2	−3	2.025	2	6	−3	2.023	4	2	3	2.029	1	−3	−1	2.029	1	−3	1	2.024
2.020	15	4	2	−1	2.021	−2	6	3	2.023	4	−2	3	2.029	3	1	1	2.029	3	−1	1	2.024
1.968	8	0	4	−2	1.965	0	−8	−2	1.964	4	0	2	1.957	2	−2	−2	1.957	2	−2	2	1.938
1.941	2	4	0	−2	1.941	−4	−4	2	1.943	4	4	2	1.957	2	−2	2	1.957	2	−2	2	1.938
1.904	6	1	5	0	1.903	2	−8	1	1.903	3	2	1	1.888	3	0	−2	1.888	3	0	2	1.862
1.879	4	4	0	2	1.880	0	0	6	1.880	0	0	6	1.880	2	2	2	1.880	2	2	2	1.938
1.837	6	2	2	3	1.836	3	−1	5	1.834	−1	3	5	1.835	2	3	0	1.835	2	3	0	1.862
		1	5	−1	1.834	1	−9	0	1.834	4	1	0	1.821	3	1	2	1.821	3	−1	−2	1.794
		5	1	0	1.829	−2	−4	5	1.831	3	2	5	1.835	3	0	2	1.835	3	0	2	1.862
1.828	6	1	5	1	1.827	3	−7	2	1.827	2	3	2	1.813	3	1	−2	1.813	3	1	−2	1.794
		2	4	−2	1.824	−1	−9	0	1.824	5	1	0	1.821	3	−2	−1	1.821	3	2	1	1.794
1.809	4	3	1	−3	1.807	4	6	0	1.807	5	−4	0	1.821	2	−3	1	1.821	2	−3	1	1.794
1.800	5	2	4	2	1.798	3	−5	4	1.797	1	3	4	1.789	3	2	1	1.789	3	2	−1	1.794
1.793	5	1	3	3	1.791	4	2	4	1.790	1	4	4	1.789	2	3	−1	1.789	2	3	1	1.794
1.781	4	5	1	−1	1.779	3	5	4	1.781	4	3	4	1.789	3	1	2	1.789	3	−1	2	1.794
1.753	26	3	1	3	1.752	2	0	6	1.751	1	2	6	1.752	2	3	1	1.752	2	3	1	1.794
		4	2	2	1.753	1	−3	6	1.753	1	1	6	1.752	3	2	1	1.752	3	2	1	1.794
		5	1	1	1.749	1	3	6	1.751	2	−1	6	1.752	3	1	2	1.752	3	1	2	1.794
1.680	2	4	4	0	1.681	0	−8	4	1.682	4	0	4	1.677	4	0	0	1.677	4	0	0	1.678
1.671	2	0	0	−4	1.670	4	4	−4	1.668	4	4	4	1.677	0	4	0	1.677	0	−4	0	1.678
1.650	12	3	5	0	1.648	1	−9	3	1.648	4	1	3	1.639	4	0	1	1.639	4	0	−1	1.628
		1	5	2	1.649	4	6	3	1.648	1	4	3	1.639	3	2	2	1.639	3	2	2	1.628
1.621	9	0	6	0	1.620	3	−9	0	1.620	3	3	0	1.606	3	0	−3	1.606	3	0	−3	1.582
1.601	14	3	3	3	1.600	−3	−9	0	1.600	6	−3	0	1.606	3	−3	0	1.606	3	−3	0	1.582
1.594	4	3	5	1	1.593	2	8	4	1.593	3	2	4	1.584	4	1	1	1.584	4	1	1	1.582
1.580	22	5	3	−1	1.580	−2	−8	4	1.582	5	2	4	1.584	4	−1	1	1.584	4	−1	1	1.582
		0	2	−4	1.580	3	−7	−4	1.578	5	3	4	1.584	1	4	1	1.584	1	−4	−1	1.582
1.562	3	2	4	3	1.561	−2	10	−1	1.560	6	2	−1	1.562	3	3	1	1.562	3	−3	−1	1.540
1.552	4	4	2	3	1.552	−4	−8	1	1.552	6	4	1	1.562	3	3	1	1.562	3	−3	1	1.540
1.532	6	2	6	0	1.530	2	10	2	1.530	4	2	2	1.519	4	0	−2	1.519	4	0	−2	1.501
1.517	2	4	4	2	1.517	−2	−10	2	1.517	6	−2	2	1.519	4	−2	0	1.519	4	−2	0	1.501
1.512	3	2	2	−4	1.511	−4	−8	−2	1.510	6	4	2	1.519	2	4	0	1.519	2	−4	0	1.501
1.488	10	3	5	−2	1.488	−1	11	1	1.489	6	−1	1	1.486	4	−2	−1	1.486	4	−2	−1	1.465
		4	4	2	1.487	2	−6	6	1.487	2	2	6	1.482	4	2	0	1.482	4	2	0	1.501
1.482	7	2	2	4	1.481	4	0	6	1.480	−2	4	6	1.482	2	4	0	1.482	2	4	0	1.501
1.479	5	6	2	0	1.478	−2	−6	6	1.480	4	−2	6	1.482	4	0	2	1.482	4	0	2	1.501
1.458	2	0	6	−2	1.458	1	−11	2	1.457	5	1	2	1.449	3	−2	−3	1.449	3	−2	−3	1.431
1.453	3	1	5	−3	1.452	−1	−11	−2	1.451	6	−1	−2	1.449	3	3	2	1.449	3	−3	−2	1.431
1.443	2	1	5	3	1.442	5	5	4	1.441	0	5	4	1.437	3	3	−2	1.437	3	3	−2	1.431
1.428	5	6	0	−2	1.426	−5	−5	4	1.428	5	−5	4	1.437	3	−2	3	1.437	3	−2	3	1.431
1.398	10	2	6	2	1.397	0	−12	0	1.397	6	0	0	1.391	4	−2	−2	1.391	4	−2	−2	1.370
1.391	5	5	1	3	1.391	1	−1	8	1.391	0	1	8	1.390	3	3	2	1.390	3	3	2	1.431
		6	0	2	1.389	−1	−1	8	1.390	1	−1	8	1.390	3	2	3	1.390	3	2	3	1.431

* Monoclinic cell, *C*2/*c*, $a_0 = 9.317\ (4)$, $b_0 = 9.720\ (4)$, $c_0 = 6.685\ (3)$ Å, $\beta_0 = 91.95\ (2)°$.

† Monoclinic or 'orthorhombic' cell, $a_4 = 9.599$, $b_4 = 16.766$, $c_4 = 11.281$ Å, $\gamma_4 = 90.84°$.

‡ Hexagonal cell, $R\bar{3}c$, $a_3 = 9.638$, $b_3 = 9.638$, $c_3 = 11.281$ Å, $\gamma_3 = 120°$.

§ Rhombohedric cell, $R\bar{3}c$, $a_2 = 6.716$ Å, $\alpha_2 = 91.70°$.

¶ Cubic cell, $a_1 = 6.713$ Å.

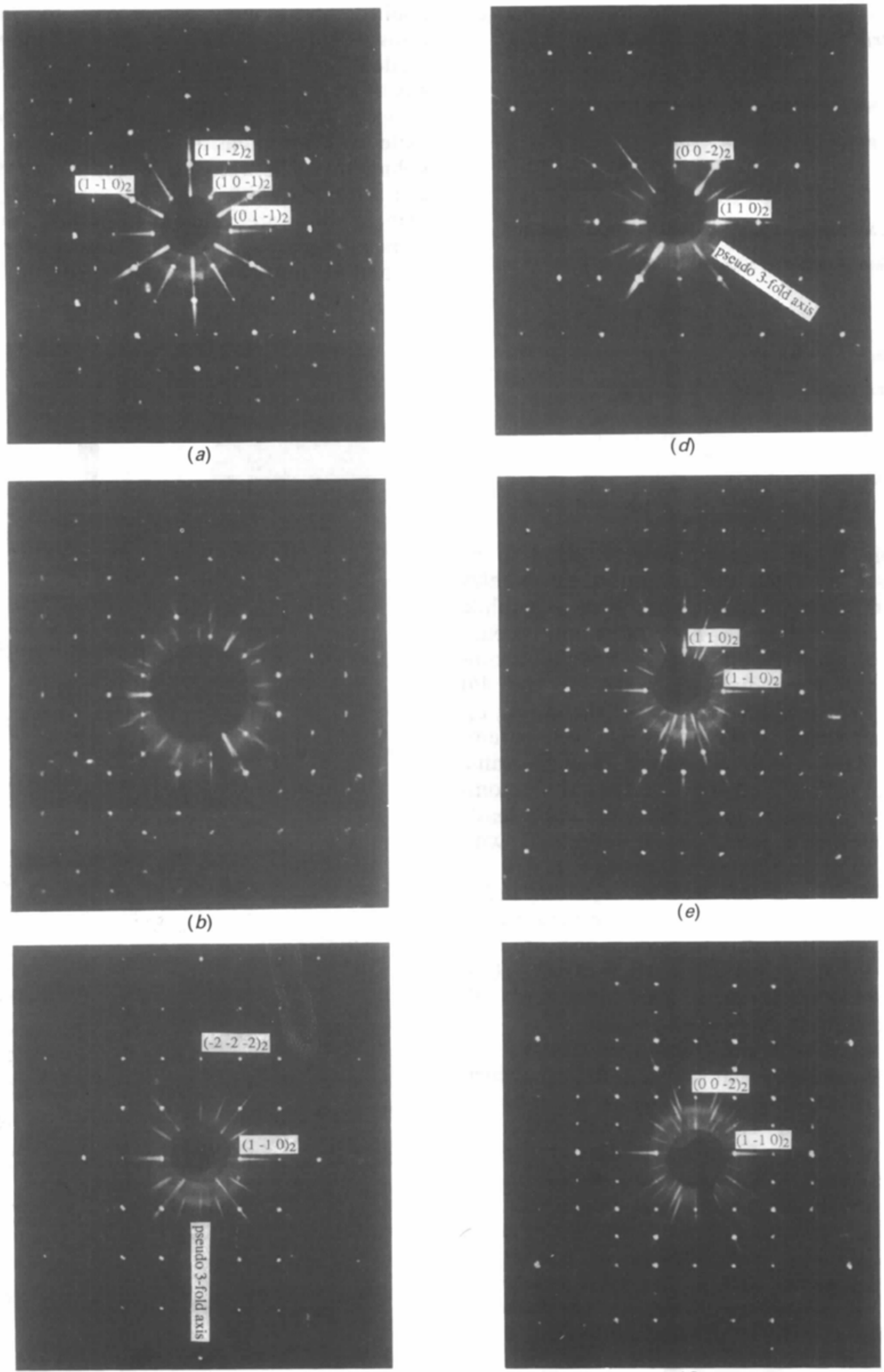

(*a*) (*d*)

(*b*) (*e*)

(*c*) (*f*)

Fig. 3. Precession photographs obtained with Zr-filtered Mo $K\alpha$ radiation on a rhombohedral-shaped crystal: (*a*) zero layer of the $[001]_3$ or $[111]_2$ zone, reflections of different individuals twinned by the rhombohedral pseudo-merohedry are nearly overlapped, (*b*) second layer of the $[001]_3$ or $[111]_2$ zone, (*c*) zero layer of the $[11\bar{2}]_2$ zone, this pattern is the same as that of (*b*), (*d*) zero layer of the $[1\bar{1}0]_2$ zone, this pattern contains the pseudo-threefold axis, (*e*) zero layer of the $[001]_2$ zone and (*f*) zero layer of the $[110]_2$ zone.

Table 2. *Transformation matrices between pseudo-symmetric lattices and the original unit cell of* Sr_3CuPtO_6

$a_0 = 9.317\ (4)$, $b_0 = 9.720\ (4)$, $c_0 = 6.685\ (3)$ Å, $\alpha_0 = 90$, $\beta_0 = 91.95\ (2)$, $\gamma_0 = 90°$

Pseudo-cubic or pseudo-rhombohedral sublattice

$$\begin{vmatrix} a_2 \\ b_2 \\ c_2 \end{vmatrix} = \begin{vmatrix} \frac{1}{2} & \frac{1}{2} & 0 \\ 0 & 0 & 1 \\ \frac{1}{2} & -\frac{1}{2} & 0 \end{vmatrix} \begin{vmatrix} a_0 \\ b_0 \\ c_0 \end{vmatrix}$$

$a_2 = 6.732$, $b_2 = 6.685$, $c_2 = 6.732$ Å, $\alpha_2 = 91.35$, $\beta_2 = 92.42$, $\gamma_2 = 91.35°$

Pseudo-rhombohedral sublattice, hexagonal setting

$$\begin{vmatrix} a_3 \\ b_3 \\ c_3 \end{vmatrix} = \begin{vmatrix} \frac{1}{2} & \frac{1}{2} & -1 \\ -\frac{1}{2} & \frac{1}{2} & 1 \\ 1 & 0 & 1 \end{vmatrix} \begin{vmatrix} a_0 \\ b_0 \\ c_0 \end{vmatrix}$$

$a_3 = 9.599$, $b_3 = 9.599$, $c_3 = 11.281$ Å, $\alpha_3 = 89.88$, $\beta_3 = 90.12$, $\gamma_3 = 119.16°$

Pseudo-monoclinic sublattice (close to orthorhombic)

$$\begin{vmatrix} a_4 \\ b_4 \\ c_4 \end{vmatrix} = \begin{vmatrix} -\frac{1}{2} & \frac{1}{2} & 1 \\ -\frac{1}{2} & -\frac{3}{2} & 1 \\ 1 & 0 & 1 \end{vmatrix} \begin{vmatrix} a_0 \\ b_0 \\ c_0 \end{vmatrix}$$

$a_4 = 9.599$, $b_4 = 16.766$, $c_4 = 11.281$ Å, $\alpha_4 = 89.93$, $\beta_4 = 89.88$, $\gamma_4 = 90.84°$

The ellipsoid, which was nonetheless found to be twinned, was mounted on an automatic Nonius four-circle diffractometer equipped with a graphite monochromator and Ag $K\alpha$ radiation. Long-exposure precession photographs showed that it consisted of only two individuals (Figs. 4*a* and 4*b*) generated by the pseudo-symmetry of the (a_4, b_4, c_4) pseudo-orthohexagonal sublattice. The cell parameters of this lattice were determined from the same single crystal mounted on the automatic diffractometer for the intensity data collection. The least-squares refinement applied to 20 reflections with large Bragg angle gave $a_4 = 9.598\ (6)$, $b_4 = 16.770\ (7)$, $c_4 = 11.280\ (6)$ Å, $\alpha_4 = 90$, $\beta_4 = 90$, $\gamma_4 = 90.81\ (5)°$. The $C2/c$ cell parameters, deduced from these values with the appropriate matrix transformation, are $a_0 = 9.328$, $b_0 = 9.720$, $c_0 = 6.678$ Å, $\alpha_0 = 90.02$, $\beta_0 = 92.01$, $\gamma_0 = 89.98°$. They are in good agreement with those obtained from the powder pattern.

The intensities were collected (ω–2θ scans) using the pseudo-orthohexagonal cell (a_4, b_4, c_4), which allowed the reflections from the two twin individuals to be easily measured. To apply the twin correction, all possible reflections of both individuals were measured. Three standard reflections were monitored to keep a running check on the crystal orientation. The corresponding correction factor varied in the range 0.969–1.003. Lorentz and polarization corrections were applied together with an empirical absorption correction for whose application a transmission curve was deduced from ψ-scan measurements ($\mu = 282.1\ \mathrm{cm}^{-1}$, the transmission factor ranged between 99.61 and 45.01%).

The structural refinements were based on the intensities of the strongest individual after the twinning correction for overlapping had been applied. Overlapping occurs only for those reflections with $l = 3n$. The two A and B individuals are related by the pseudo-mirror $(001)_4$. The total intensity of an hkl node is given by $I_{\text{total}}(hkl)_4 = I_A(hkl)_4 + I_B(hk\bar{l})_4$. In the non-zero levels with $l_4 = 3n$, approximate twin-free intensities can be obtained. If R is the volume ratio between the B and A individuals, one can write $I_{\text{total}}(hkl)_4 = I_A(hkl)_4 + RI_A(hk\bar{l})_4$. As the twin fractions are different from 50%, simple arithmetic allows the separation of measured intensities at hkl and $hk\bar{l}$ into corresponding twin-free intensities.

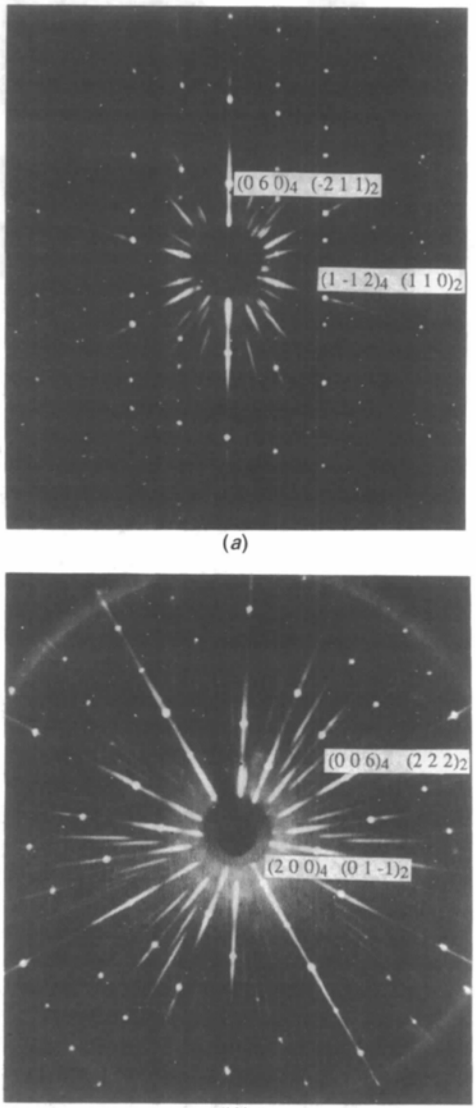

(*a*)

(*b*)

Fig. 4. Precession photograph obtained with Zr-filtered Mo $K\alpha$ radiation on the crystal used for the data collection: (*a*) zero layer of the $[\bar{2}01]_4$ zone, showing the twinning by reticular pseudo-merohedry and (*b*) zero layer of the $[010]_4$ zone. The plane of the figure is the twinning plane and reflections of both individuals are almost exactly overlapped.

Table 3. *Positional and thermal parameters for* Sr_3CuPtO_6

	x	y	z	β_{11} or B_{iso}	β_{22}	β_{33}	β_{12}	β_{13}	β_{23}
Pt	$\frac{1}{4}$	$\frac{1}{4}$	$\frac{1}{2}$	0.00076 (9)	0.00047 (8)	0.0012 (2)	0.0001 (1)	0.0001 (2)	0.0004 (2)
Cu	0.0	0.2987 (4)	$\frac{1}{4}$	0.0012 (3)	0.0029 (3)	0.0015 (6)	0.0	−0.0005 (8)	0.0
Sr(1)	0.0	0.8968 (2)	$\frac{1}{4}$	0.0005 (2)	0.0006 (2)	0.0018 (4)	0.0	0.0002 (5)	0.0
Sr(2)	0.3145 (2)	0.0727 (2)	0.1211 (2)	0.0009 (1)	0.0008 (1)	0.0012 (3)	−0.0007 (3)	−0.0001 (4)	0.0001 (4)
O(1)	0.288 (1)	0.815 (1)	0.285 (2)	0.4 (2)					
O(2)	0.058 (1)	0.341 (1)	0.537 (2)	0.6 (2)					
O(3)	0.141 (1)	0.073 (1)	0.427 (2)	0.7 (2)					

Table 4. *Thermal data for* Sr_3CuPtO_6

			Angles (°) with		
		R.m.s. (Å)	x	y	z
Pt	r_1	0.059	29.6	69.4	69.7
	r_2	0.055	118.5	64.9	39.7
	r_3	0.043	97.1	33.4	122.4
Cu	r_1	0.118	89.9	0.0	90.0
	r_2	0.075	22.6	90.1	112.6
	r_3	0.055	67.4	90.0	22.6
Sr(1)	r_1	0.064	83.9	89.9	6.1
	r_2	0.055	88.3	1.7	90.3
	r_3	0.049	6.3	91.7	96.1
Sr(2)	r_1	0.074	44.0	132.8	98.3
	r_2	0.051	80.4	91.8	9.8
	r_3	0.048	47.6	42.8	95.3
O(1)	r	0.074	—		—
O(2)	r	0.085	—	—	
O(3)	r	0.091	—	—	...

From the A/B intensity ratio for the non-overlapped reflections ($l \neq 3n$), it was determined that the two individuals occupied 78.7 and 21.3% of the crystal volume, respectively ($R = 0.27$). All the reflections, included in the entire Ewald sphere for $0 < \sin\theta/\lambda < 0.61$ Å^{-1} (h $-12 \rightarrow 12$, k $-21 \rightarrow 21$, l $-14 \rightarrow 14$), were measured. The large pseudo-orthorhombic cell (a_4, b_4, c_4) controlling the twinning was used. From 10 627 measured reflections, 3517 had $I > 2\sigma(I)$ and were considered as observed. Of these observed reflections, 766 belong to both individuals while 1513 do not overlap and belong to the larger A individual. The average difference (2.1%) in intensity between Friedel pairs was found to be larger than expected. This was due to either the absence of the symmetry center from the structure or to an inaccurate absorption correction. As stated above, the shape of the sample was an irregular ellipsoid containing two individuals whose domains are distributed at random, thus the absorption varied with the orientation. We believe that the most probable cause of the difference between the intensity of Friedel pairs was due to the inaccuracy of the absorption correction. After averaging in the monoclinic point group $2/m$, the total number of independent reflections was 582 and the agreement factor of averaging among equivalent reflections was 2.6%.

The structure was determined by the use of three-dimensional Patterson series as well as direct methods. Refinements were carried out using the *SDP* package (Enraf–Nonius, 1979). The f curves for neutral Sr, Cu and Pt were taken from *International Tables for X-ray Crystallography* (1974, Vol. IV). The anomalous-dispersion coefficients of Cromer & Liberman (1970) were used. Various weighting schemes were tried and the unit-weight scheme was found to give the best results as it took into account the weak deformation from the trigonal average structure.

Although the reflections related by the monoclinic symmetry had the same intensity, structural refinements with a triclinic pseudo-cubic cell (a_2, b_2, c_2) were tried and yielded $R = 0.053$, $wR = 0.058$ for the 1086 independent reflections. The atomic positions related by the $2/c$ symmetry elements and transformed in the (a_0, b_0, c_0) cell were within the respective standard deviations. Very weak reflections with $I < 10^{-3}I_{max}$, at low Bragg angles, were not taken into account by this cell. Refinements in a

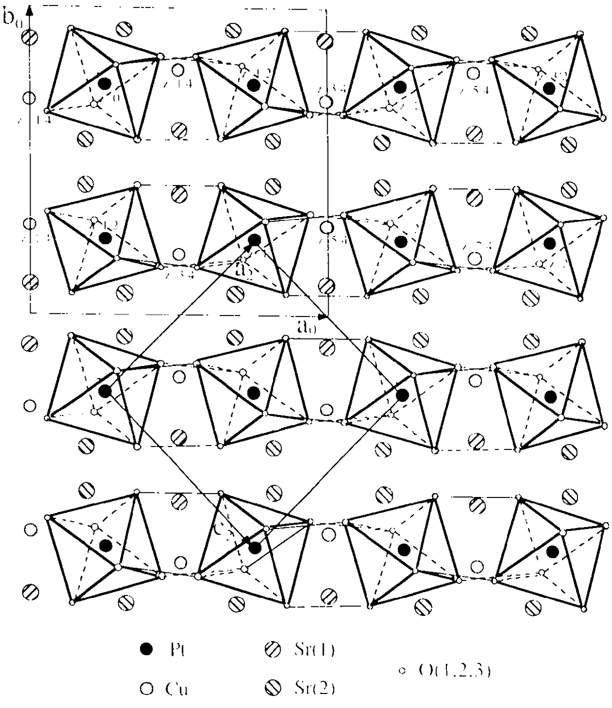

Fig. 5. Projection of the structure along the $[001]_0$ or $[010]_2$ direction, showing the coordinations of Pt and Cu sites in Sr_3CuPtO_6. Only the O—O bonds belonging to the PtO_6 octahedra and CuO_6 trigonal prisms are drawn. Pt black full circles; Cu grey full circles; Sr(1,2) hatched circles; O(1,2,3) small open circles.

Table 5. *Distances* (Å) *and angles* (°) *in* Sr_3CuPtO_6

Pt—O(1)	2.028 (14)	× 2	Cu—O(1)	2.007 (14)	× 2
Pt—O(2)	2.016 (15)	× 2	Cu—O(2)	2.017 (14)	× 2
Pt—O(3)	2.046 (15)	× 2	Cu—O(3)	2.800 (15)	× 2
O(1)—Pt—O(2)	98.40	× 2	O(1)—Cu—O(2)	96.10	× 2
O(1)—Pt—O(2)	81.60	× 2	O(1)—Cu—O(2)	82.08	× 2
O(1)—Pt—O(3)	91.81	× 2	O(1)—Cu—O(3)	117.61	× 2
O(1)—Pt—O(3)	88.19	× 2	O(1)—Cu—O(3)	70.07	× 2
O(2)—Pt—O(3)	92.10	× 2	O(2)—Cu—O(3)	131.87	× 2
O(2)—Pt—O(3)	87.90	× 2	O(2)—Cu—O(3)	69.48	× 2
Sr(1)—O(1)	2.798 (14)	× 2	Sr(2)—O(1)	2.751 (14)	
Sr(1)—O(2)	2.775 (15)	× 2	Sr(2)—O(1)	2.502 (14)	
Sr(1)—O(3)	2.443 (15)	× 2	Sr(2)—O(1)	2.622 (14)	
Sr(1)—O(3)	2.585 (15)	× 2	Sr(2)—O(2)	2.775 (15)	
			Sr(2)—O(2)	2.503 (15)	
			Sr(2)—O(2)	2.676 (14)	
			Sr(2)—O(3)	2.646 (15)	
			Sr(2)—O(3)	2.480 (15)	

Table 6. *Bond strengths and valences*

	O(1)	O(2)	O(3)	Total valence
Pt	2 × 0.669	2 × 0.690	2 × 0.637	3.992
Cu	2 × 0.412	2 × 0.401	2 × 0.048	1.722
Sr(1)	2 × 0.159	2 × 0.169	2 × (0.415 + 0.283)	2.052
Sr(2)	(0.181 + 0.354 + 0.256)	(0.169 + 0.353 + 0.221)	(0.240 + 0.376)	2.150
Total valence	2.031	2.003	1.999	12.066

face-centered triclinic space group with a larger cell were tried but the results were not conclusive. The refinement of the average structure in the space group $R\bar{3}c$ with the rhombohedral cell, (a_2, b_2, c_2) or (a_3, b_3, c_3) ($R \simeq 24\%$), was totally inconclusive. The best refinement was carried out with the monoclinic cell (a_0, b_0, c_0) and the space group $C2/c$. The final full-matrix least-squares refinement (based on F) was carried out with the space group $C2/c$ and 582 independent reflections. The scale factor, 14 positional parameters, 20 anisotropic thermal parameters for the cations, three isotropic thermal parameters for the anions and the isotropic secondary-extinction parameter [$g = 3.0\,(3) \times 10^{-7}$] were varied simultaneously. The R factors were $R = 0.048$, $wR = 0.054$, with maximum $\Delta/\sigma = 0.01$. The corresponding positional and thermal parameters are given in Table 3. The maximum peak height in the difference Fourier maps was 1.57 e Å^{-3}. The chemical formula was found to be Sr_3CuPtO_6.

When occupancy factors were varied during the refinement, only those of Pt and Cu decreased to 0.90 and 0.95, respectively, but the R and wR factors decreased only slightly to 0.047 and 0.052. The difference Fourier maps calculated after the refinements with isotropic thermal factors in space group $C2/c$ showed weak peaks (2 e Å^{-3}) very close to the Cu position at (0.0, 0.23, 0.25). After the final refinement whose results are reported in Table 3, the Cu atoms exhibited the largest anisotropic thermal factors, with the major axis along the b direction (Table 4). These results indicate that some disorder and/or cation substitution could exist in the sample which would induce an additional distortion. The disorder is probably related to the trigonal twinning which affects mainly the Cu positions (see below). The additional distortion would be responsible for the few very weak reflections which were not taken into account by using the $C2/c$ cell.

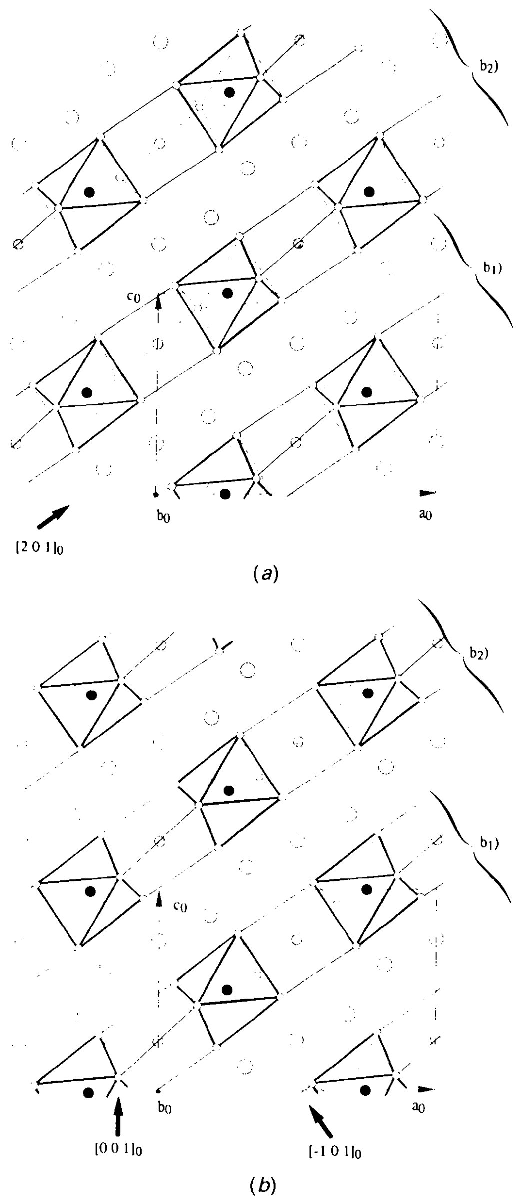

Fig. 6. Projection of the structure of Sr_3CuPtO_6 along the $[0\bar{1}0]_0$ or $[\bar{1}01]_2$ direction, showing isolated $[111]_2$ rows of PtO_6 octahedra and CuO_6 trigonal prisms. Only the O—O bonds belonging to these cations are drawn: (a) all atoms with $0 < y < 1/2$ and (b) all atoms with $1/2 < y < 1$. Pt small black full circles; Cu small grey circles; Sr(1,2) large grey circles; O(1,2,3) small open circles.

Description of the structure

A projection of the Sr_3CuPtO_6 structure on the a_0c_0 plane is shown in Fig. 5. The positional parameters together with the unit-cell dimensions determined from the X-ray powder data gave the interatomic distances and angles reported in Table 5. The Pt atoms are in the special positions 4(*d*) of the space group *C*2/*c*, at the symmetry center. The PtO_6 octahedra are quite regular with Pt—O distances ranging from 2.02 to 2.05 Å, in agreement with previously observed $^{\mathrm{VI}}\mathrm{Pt}^{4+}$—O distances. For example, the $^{\mathrm{VI}}$Pt—O distances in Sr_4PtO_6 and in MPt_3O_6 (M = Mn, Co, Zn, Mg, Cd) vary between 2.00 and 2.03 Å (Randall & Katz, 1959; Schwartz *et al.*, 1983). The $^{\mathrm{VI}}$Pt—O angles in the title compound are closer to 90° [Δ(O—Pt—O) < 8.4°] than in these other compounds [Δ(O—Pt—O) = 11–13°]. The rigid nature of the PtO_4 squares and PtO_6 octahedra is a common feature of most Pt^{2+} or Pt^{4+} oxides.

The Cu cations are in the special positions 4(*e*) on the twofold axis. They are surrounded by six O atoms arranged as a distorted trigonal prism. Since they are displaced from the pseudo-threefold axis of the pseudo-trigonal cell (a_2, b_2, c_2), towards one of the rectangular faces of the trigonal prism (Figs. 5, 6 and 7), there exist two types of Cu—O distances: four ranging between 2.01 and 2.02 Å and two at about 2.80 Å. These four shortest distances are still too long for $^{\mathrm{IV}}\mathrm{Cu}^{2+}$ cations. An additional displacement (as indicated by the large thermal parameters of the Cu cations) of about 0.2 Å towards the prism square would result in four shorter Cu—O distances (1.99–2.00 Å) which would be more reasonable for $^{\mathrm{IV}}\mathrm{Cu}^{2+}$ cations.

The structure of Sr_3CuPtO_6 contains edge-sharing chains of alternating PtO_6 octahedra and CuO_4 'squares' along the $[111]_2$ pseudo-threefold axis (Fig. 6). The chains are linked together by Sr—O bonds. The Sr cations are in eightfold coordination with the Sr—O distances varying between 2.44 and 2.80 Å.

The size of the 4(*e*) sites is such that Pt^{2+} cations, if they existed, could be easily located in these sites. The square coordination with four short Pt—O distances (1.94–2.00 Å) would be quite reasonable for Pt^{2+} cations (Randall & Katz, 1959; Schwartz & Prewitt, 1984; Schwartz *et al.*, 1983; Schwartz,

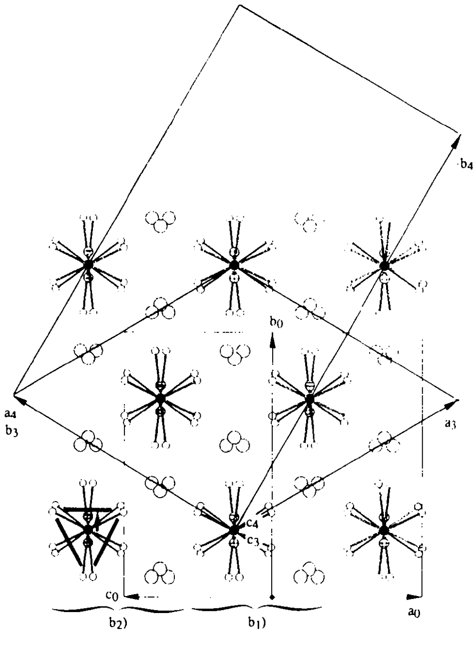

(*a*)

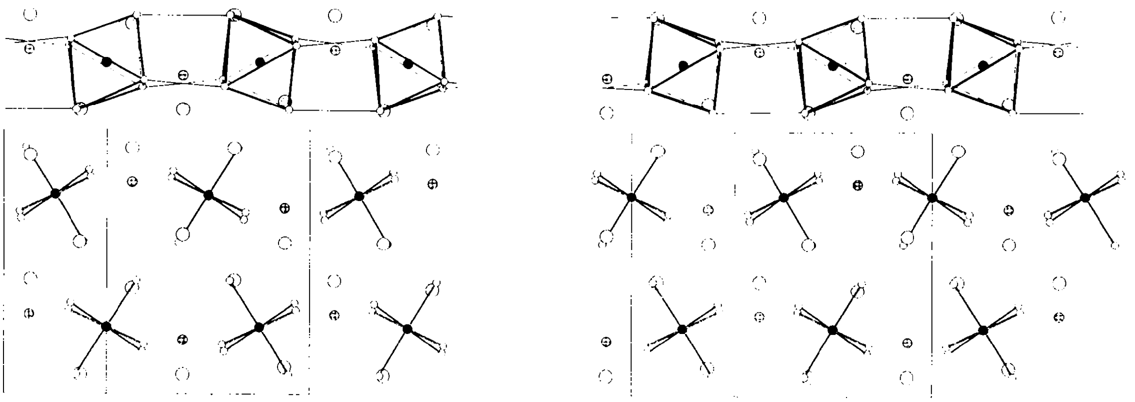

(b_1) (b_2)

Fig. 7. Projections of the Sr_3CuPtO_6 structure. Only the Pt—O bonds belonging to the PtO_6 octahedra are drawn. (*a*) Along the $[001]_3$ ($\longleftrightarrow [111]_2$ or $\longleftrightarrow [201]_0$) direction, with the pseudo-threefold axis perpendicular to the projection plane, going through Pt cations. One trigonal prism around one of the Cu cations is drawn and the corresponding displacement is indicated by an arrow. Two pseudo-symmetric cells are outlined. (*b*) Along the $[\bar{1}01]_0$ direction. Only the atoms corresponding to two layers perpendicular to the projection are shown: (b_1) corresponds to the layers indicated by b_1 in Fig. 6 and in (*a*), and (b_2) corresponds to the layers indicated by b_2 in Fig. 6 and in (*a*). Pt small black full circles; Cu small grey circles; Sr(1,2) large grey circles; O(1,2,3) small open circles.

Parise, Prewitt & Shannon, 1982). On the other hand, the Pt^{4+} cations of the 4(*d*) sites could be replaced either by Cu^{2+} cations with a small distortion and a contraction of the cation—O distances or by Bi^{5+} cations with a small increase of the site size. If the occupancy parameter of the 4(*d*) site indicated that the first substitution was not probable, the second is not easy to reveal because Bi and Pt cations have similar scattering factors. For this reason we checked the structural electroneutrality by calculating individual bond strengths.

The cation–anion bond strengths can be estimated from empirical formulae which are the extrapolation of the Pauling rules. The relationship of Brown & Altermatt (1985) was used: $s = \exp[(d_0 - d)/B]$, where s and d are the bond strength and bond length, respectively, and d_0 and B are two constants for the given cation–anion distance. The sum of the bond strengths, $\sum_i s(\text{cation—O}_i)$, must be equal to the cation valence, and the sum of the bond strengths, $\sum_j s(\text{cation}_j\text{—O})$, must be equal to the O valence. The B constant was taken as 0.37 and the d_0 distances used were $d_0(Pt^{4+}\text{—O}) = 1.879$, $d_0(Cu^{2+}\text{—O}) = 1.679$, $d_0(Sr^{2+}\text{—O}) = 2.118$, $d_0(Pt^{2+}\text{—O}) = 1.772$, $d_0(Bi^{5+}\text{—O}) = 2.02$ and $d_0(Bi^{3+}\text{—O}) = 2.094$ Å. A good agreement is only obtained for the composition Sr_3CuPtO_6, *i.e.* with only P on the 4(*d*) site and only Cu on the 4(*e*) sites. Calculated bond strengths and valences are given in Table 6.

The structure of Sr_3CuPtO_6 described in monoclinic *C*2/*c* can be related to that of other M_4PtO_6 compounds:

(i) Sr_4PtO_6 has $R\bar{3}c$ symmetry with hexagonal cell parameters [$a = 9.740\,(2)$, $c = 11.900\,(2)$ Å], which are very close to those of the (a_3, b_3, c_3) unit cell for Sr_3CuPtO_6. The main difference between the structure of Sr_3CuPtO_6 and that of Sr_4PtO_6 concerns the stacking of octahedral PtO_6 groups which takes place *via* the Cu sites in the former and *via* the Sr sites in the latter. The change in shape of this site (Cu or Sr) corresponds to a change in symmetry and consequently different crystal symmetries are obtained. In the structure of Sr_4PtO_6 the Sr cations are surrounded by regular trigonal O prisms (Randall & Katz, 1959; Ben-Dor *et al.*, 1983).

(ii) Ba_4PtO_6 is isostructural with the previous compound [$R\bar{3}c$, $a = 10.2102\,(2)$, $c = 12.6172\,(2)$ Å]. The BaO_6 trigonal prisms are also quite regular (Wilkinson & Cheetham, 1989). During the course of this study, Wilkinson and coworkers pointed out the close relationship between Sr_3CuPtO_6 and Ba_4PtO_6 (Wilkinson & Cheetham, 1989; Wilkinson, Cheetham, Kunnmann & Kvick, 1991).

(iii) Ca_4PtO_6 has been reported to exist with two polymorphs, one trigonal ($R\bar{3}c$, $a \simeq 9.18$, $c \simeq 11.25$ Å) (McDaniel, 1972) and one orthorhombic (*Cmcm*, $a = 9.18$, $b = 9.24$, $c = 6.50$ Å) (Czaya, 1970). The latter cell is similar to the monoclinic (a_0, b_0, c_0) cell of Sr_3CuPtO_6.

The space group *C*2/*c* of Sr_3CuPtO_6 is a sub-group of *Cmcm*, which itself is derived from the space group $R\bar{3}c$ with an adequate cell transformation. These examples show the close structural relationships among the M_4PtO_6 compounds. The pseudo-lattices are related to the unit cell with the highest symmetry by means of the transformation matrices given in Table 2.

As shown in the $[001]_3$ projection in real space (see Fig. 7*a*), the main difference between the monoclinic *C*2/*c* structure of Sr_3CuPtO_6 and the $R\bar{3}c$ structure is the position of the Cu cations, which are displaced in the former compound by 0.41 Å towards one face of the CuO_6 trigonal prism and nearly have a square coordination (see Fig. 7*a*). When, in the space group *C*2/*c*, isotropic thermal factors were used, weak peaks at the position (0.0, 0.23, 0.25) close to the center of the trigonal prism were observed in difference Fourier maps. As rhombohedral twinning mainly affects the Cu position, these peaks were due to the different twin individuals. Consequently, the refinement would have resulted in a Cu position which is too close to the center of the trigonal prism, corresponding to an underbonded Cu cation. Calculated Cu valences for the Cu cation either placed at the center of the trigonal prism or at the center of the 'square' face are 1.43+ and 1.77+, respectively. Unlike the Sr^{2+} cations, the Cu^{2+} cations prefer the 'square' coordination, so that the *C*2/*c* symmetry is intrinsically due to the presence of Cu in Sr_3CuPtO_6 and the trigonal symmetry is intrinsic to the Sr_4PtO_6 compound.

Usually the crystals of Sr_3CuPtO_6 have a hexagonal platelet-like habit corresponding to the (a_3, b_3, c_3) pseudo-rhombohedral lattice. This indicates that this lattice, which is responsible for twinning, also controls the crystal morphology. Nearly the same crystal shape is obtained for the $R\bar{3}c$ Ca_4PtO_6 compound (Ohsato, Sugimura & Kageyama, 1981).

References

Akimitsu, J., Yamazaki, A., Sawa, H. & Fujiki, H. (1988). *Jpn J. Appl. Phys.* **27**, L2080.

Ben-Dor, L., Suss, J. T. & Cohen, S. (1983). *J. Cryst. Growth*, **64**, 395–396.

Brown, I. D. & Altermatt, D. (1985). *Acta Cryst.* **B41**, 244–247.

Chamberland, B. L. & Silverman, S. (1979). *J. Less Common Met.* **65**, P41–P48.

Cromer, D. T. & Liberman, D. (1970). *J. Chem. Phys.* **53**, 1891–1898.

Czaya, Z. (1970). *Z. Anorg. Allg. Chem.* **375**, 61–64.

Enraf–Nonius (1979). *Structure Determination Package.* Enraf–Nonius, Delft, The Netherlands.

Friedel, G. (1964). *Leçons de Cristallographie.* Paris: Blanchard.

Ikeda, Y., Ito, H., Shimomura, S., Oue, Y., Inaba, K., Hiroi, K. & Takano, M. (1989). *Physica*, **C159**, 93–104.

McDaniel, C. L. (1972). *J. Am. Ceram. Soc.* **55**, 426–427.
Maeda, H., Tanaka, Y., Fukutomi, M. & Asano, T. (1988). *Jpn J. Appl. Phys.* **27**, L209.
Michel, C., Hervieu, M., Borel, M. M., Grandin, A., Deslandes, F., Provost, J. & Raveau, B. (1987). *Z. Phys.* **B68**, 421–424.
Ohsato, H., Sugimura, T. & Kageyama, K. (1981). *J. Cryst. Growth*, **51**, 1–5.
Randall, J. J. & Katz, L. (1959). *Acta Cryst.* **12**, 519–521.
Randall, J. J. & Ward, R. (1969). *J. Am. Chem. Soc.* **81**, 2629–2631.
Roth, R. S., Rawn, C. J. & Bendersky, L. A. (1990). *J. Mater. Res.* **5** (1), 46–52.
Roth, R. S., Rawn, C. J., Burton, B. P. & Beech, F. (1990*a*). *J. Res. NIST*, March- April.
Roth, R. S., Rawn, C. J., Burton, B. P. & Beech, F. (1990*b*). *J. Res. NIST*, May–June.
Saggio, J. A., Sujata, K., Hahn, J., Hwu, S. J., Poeppelmeier, K. R. & Mason, T. O. (1989). *J. Am. Ceram. Soc.* **72**(5), 849-853.
Schneider, S. J. & McDaniel, C. L. (1969). *J. Am. Ceram. Soc.* **52**(9), 518–519.
Schwartz, K. B., Parise, J. B., Prewitt, C. T. & Shannon, R. D. (1982). *Acta Cryst.* **B38**, 2109–2116.
Schwartz, K. B., Parise, J. B., Prewitt, C. T. & Shannon, R. D. (1983). *Acta Cryst.* **B39**, 217–226.
Schwartz, K. B. & Prewitt, C. T. (1984). *J. Phys. Chem. Solids*, **45**(1), 1–21, and references therein.
Schwartz, K. B., Prewitt, C. T., Shannon, R. D., Corliss, L. M., Hastings, J. M. & Chamberland, B. L. (1982). *Acta Cryst.* **B38**, 363–368.
Strobel, P., Kelleher, K., Holtzberg, F. & Worthington, T. (1988). *Physica*, **C156**, 343–440.
Tu, H. Y., Hodeau, J. L., Bordet, P., Chandrashekhar, G. V., Fournier, T., Strobel, P. & Marezio, M. (1990). *Acta Cryst.* **A46**, C-336.
Wilkinson, A. P. & Cheetham, A. K. (1989). *Acta Cryst.* **C45**, 1672–1674.
Wilkinson, A. P., Cheetham, A. K., Kunnmann, W. & Kvick, A. (1991). In the press.

Acta Cryst. (1992). **B48**, 11–16

Structure Refinement of Al_3Zr using Single-Crystal X-ray Diffraction, Powder Neutron Diffraction and CBED

By Y. Ma

Department of Physics, University of Oslo, 1048 *Blindern,* 0316 *Oslo* 3, *Norway*

C. Rømming

Department of Chemistry, University of Oslo, 1033 *Blindern,* 0315 *Oslo* 3, *Norway*

B. Lebech

*Risø National Laboratory, DK-*4000 *Roskilde, Denmark*

and J. Gjønnes and J. Taftø

Department of Physics, University of Oslo, 1048 *Blindern,* 0316 *Oslo* 3, *Norway*

(*Received* 27 *June* 1991; *accepted* 2 *September* 1991)

Abstract

The structure of the intermetallic compound Al_3Zr has been studied at 293 K by single-crystal X-ray diffraction (Mo $K\alpha$ radiation, $\lambda = 0.71069$ Å), powder neutron diffraction $\{\lambda[\mathrm{Ge}(711)] = 1.0867$ Å$\}$ and convergent-beam electron diffraction (CBED) (200 keV, $\lambda = 0.0251$ Å). The structure of Al_3Zr comprises four close-packed metal sub-lattices and has the tetragonal space group $I4/mmm$ with $a = 3.9993\ (5)$, $c = 17.283\ (2)$ Å, $V = 276.43\ (6)$ Å^3, $Z = 4$, $D_x = 4.136$ g cm^{-3}, $\mu = 45.11$ cm^{-1}. The new z coordinates of four Al and four Zr atoms on the e position [$z_{\mathrm{Al}(e)}$ and $z_{\mathrm{Zr}(e)}$] were determined by single-crystal X-ray diffraction: $z_{\mathrm{Al}(e)} = 0.37498\ (5)$ and $z_{\mathrm{Zr}(e)} = 0.11886\ (1)$. The results from single-crystal X-ray diffraction were confirmed by powder neutron diffraction, although they differ considerably from previously reported data [Brauer (1939). *Z. Anorg. Chem.* **242**, 1–22] and differ in parts from the CBED work. The structure was refined to $R = 0.016$, $wR = 0.021$ for 304 unique observed reflections for single-crystal X-ray diffraction, while it was refined to $R = 0.064$, $wR = 0.095$ for 43 resolved peaks for powder neutron diffraction. A large anisotropic effect for the temperature factor of the Al atoms on the e position [Al(e)] was found by single-crystal X-ray diffraction, which may have both thermal and non-thermal origins. For the newly proposed CBED technique, a wide cone of incident rays was used to obtain inten-

0108-7681/92/010011-06$03.00